

Reduced extracellular space in the brain of tenascin-R- and HNK-1-sulphotransferase deficient mice

Eva Syková,^{1,2} Ivan Voříšek,^{1,2} Tomáš Mazel,^{1,2} Tatiana Antonova^{1,†} and Melitta Schachner³

¹Institute of Experimental Medicine, Academy of Sciences of the Czech Republic, Vídeňská 1083, 142 20 Prague 4, Czech Republic

²Department of Neuroscience and Center for Cell Therapy and Tissue Repair, Charles University, 2nd Medical Faculty, V úvalu 84, 150 06 Prague 5, Czech Republic

³Zentrum für Molekulare Neurobiologie, University of Hamburg, Falkenried 94, D-20251, Hamburg, Germany

Keywords: diffusion, extracellular matrix, hippocampus, magnetic resonance, tenascin-C, tortuosity

Abstract

Tenascin-R (TN-R), a large extracellular glycoprotein, is an important component of the adult brain's extracellular matrix (ECM); tenascin-C (TN-C) is expressed mainly during early development, while human natural killer 1 (HNK-1) is a sulphated carbohydrate epitope that attaches to these molecules, modifying their adhesive properties. To assess their influence on extracellular space (ECS) volume and geometry, we used the real-time iontophoretic method to measure ECS volume fraction α and tortuosity λ , and diffusion-weighted magnetic resonance imaging (MRI) to measure the apparent diffusion coefficient of water (ADC_w). Measurements were performed *in vivo* in the cortex and CA1 hippocampal region of TN-R-, TN-C- and HNK-1 sulphotransferase (ST)-deficient adult mice and their wild-type littermate controls. In both cortex and hippocampus, the lack of TN-R or HNK-1 sulphotransferase resulted in a significant decrease in α and λ . Compared with controls, α in TN-R^{-/-} and ST^{-/-} mice decreased by 22–26% and 9–15%, respectively. MRI measurements revealed a decreased ADC_w in the cortex, hippocampus and thalamus. ADC_w reflected the changes in α ; the decrease in λ indicated fewer diffusion obstacles in the ECS, presumably due to a decreased macromolecular content. No significant changes were found in TN-C^{-/-} animals. We conclude that in TN-R^{-/-} and ST^{-/-} mice, which show morphological, electrophysiological and behavioural abnormalities, the ECS is reduced and its geometry altered. TN-R, as an important component of the ECM, appears to maintain an optimal distance between cells. The altered diffusion of neuroactive substances in the brain will inevitably affect extrasynaptic transmission, neuron–glia interactions and synaptic efficacy.

Introduction

Three tenascins (TN-C, TN-R and TN-Y), large extracellular matrix (ECM) glycoproteins, have been found in brain tissue (Joester & Faissner, 2001). TN-C is expressed mainly during early development and tissue remodelling in neural and non-neural tissues (Jones & Jones, 2000). In adulthood, TN-C expression persists in areas known to display a high degree of functional plasticity, such as the hippocampus or hypothalamus (Theodosios *et al.*, 1997; Nakic *et al.*, 1998). By contrast, TN-R is expressed later in ontogenesis, mainly by myelinating oligodendrocytes (Bartsch *et al.*, 1993), and its neuronal expression persists until adulthood (Fuss *et al.*, 1993). Together with chondroitin sulphate proteoglycans, TN-R is a critical component of perineuronal nets surrounding neurons in various parts of the brain, including the cerebral cortex and hippocampus (Härtig *et al.*, 1992; Brückner *et al.*, 2000). The functional roles of tenascin molecules are manifold, being, for instance, involved in the regulation of neurite outgrowth (Schachner *et al.*, 1994; Pesheva & Probstmeier, 2000). TN-R-deficient mice (TN-R^{-/-}) mice (Saga *et al.*, 1992; Weber *et al.*, 1999) have a reduced body weight, small size and a low pregnancy

rate. They show locomotor hyperactivity, alterations in dopaminergic transmission in the brain and paradoxical responses to dopamine agonists (Fukamauchi *et al.*, 1997). At the microscopic level, staining for chondroitin sulphate proteoglycans and perineuronal nets is weak and abnormally distributed (Weber *et al.*, 1999; Haunsø *et al.*, 2000). It is likely that these abnormalities lead to the decreased activity of parvalbumin-containing interneurons and reduced perisomatic inhibition of hippocampal pyramidal cells (Saghatelian *et al.*, 2001), resulting in increased basal excitatory synaptic transmission and reduced long-term potentiation (LTP; Bukalo *et al.*, 2001). TN-C-deficient mice (TN-C^{-/-}) do not show any gross anatomical abnormalities. They have subtle neurological disorders, such as deficits in coordination and hyperlocomotion. They also show reduced LTP after theta-burst stimulation, and no long-term depression after low-frequency stimulation (Evers *et al.*, 2002). HNK-1 (human natural killer 1) is a carbohydrate structure, a sulphated glucuronyl–lactosaminyl residue, attached in neural tissue to many cell adhesion molecules, including TN-R and TN-C (Bartsch *et al.*, 1993). HNK-1 is important for neuron–astrocyte and astrocyte–astrocyte adhesion (Keilhauer *et al.*, 1985). HNK-1 sulphotransferase-deficient (ST^{-/-}) mice show fewer anatomical or histological changes than TN-R^{-/-} mice, but inhibitory functions are reduced, i.e. ST^{-/-} mice show reduced perisomatic inhibition of the pyramidal cells, increased basal excitatory synaptic transmission and reduced LTP (Senn *et al.*, 2002).

Correspondence: Professor E. Syková, ¹Institute of Experimental Medicine, as above.
E-mail: sykova@biomed.cas.cz

[†]This paper is dedicated to Tatiana Antonova, recently deceased, who made a significant contribution to this study.

Received 30 March 2005, revised 5 August 2005, accepted 10 August 2005

Our previous studies revealed that the loss of ECM is accompanied by impaired spatial learning (Syková *et al.*, 2002), which can result from not only disturbed synaptic transmission, but also altered extrasynaptic 'volume' transmission mediated by extracellular space (ECS) diffusion. Therefore, in this study we investigated the ECS parameters (ECS volume and geometry) in the cortex and hippocampus of TN-R^{-/-}, ST^{-/-} and TN-C^{-/-} mice using the invasive real-time iontophoretic tetramethylammonium (TMA) method and the diffusion parameters in multiple sites in the brain using non-invasive diffusion-weighted magnetic resonance imaging (DW-MRI).

Materials and methods

Experimental animals

Animals were obtained from the breeding unit of the University Hospital Eppendorf, Hamburg, Germany. Experiments were performed in adult mice (females, aged 5–9 months) derived from heterozygous breeding of three different strains: (i) TN-R-deficient mice with a mixed C57BL/6J × 129Ola × 129Sv/Ev genetic background (TN-R^{-/-}) and wild-type littermate controls (TN-R^{+/+}) (Weber *et al.*, 1999); (ii) TN-C-deficient mice with a C57BL/6J background (TN-C^{-/-}) and their wild-type littermates (TN-C^{+/+}) (Evers *et al.*, 2002); (iii) HNK-1 ST-deficient mice with a C57BL/6J background (ST^{-/-}) and their wild-type littermates (ST^{+/+}) (Senn *et al.*, 2002). ST^{+/+} and TN-C^{+/+} mice are identical from the point of view of both their genetic background and our handling of them in this study. Although we use the terms TN-C^{+/+} and ST^{+/+} in the text, both terms in fact refer to a single group.

Experiments were carried out in accordance with the European Communities Council Directive of 24 November 1986 (86/609/EEC). All efforts were made to minimize the number of animals used.

Measurements of ECS diffusion parameters using the real-time iontophoretic TMA method

The diffusion of substances in brain tissue obeys Fick's laws, when modified by three diffusion parameters: the ECS volume fraction (α = ECS volume/total tissue volume); ECS tortuosity λ ($\lambda^2 = D/ADC$, where D is the diffusion coefficient of a substance in free solution and ADC its apparent diffusion coefficient in the tissue); and k' representing non-specific uptake from the ECS (Nicholson & Phillips, 1981; Nicholson & Syková, 1998). Therefore, volume fraction α describes the relative size of the ECS, and tortuosity λ can be interpreted as an increase in diffusion path length due to all the obstacles encountered within the ECS, e.g. cellular structures or ECM macromolecules. The ECS diffusion parameters, i.e. α , λ and k' , were measured *in vivo* using TMA-selective microelectrodes (real-time iontophoretic TMA method), as described previously (Voříšek & Syková, 1997a). Briefly, TMA cations (TMA^+), to which cell membranes are relatively impermeable, were released by iontophoresis from a microelectrode and their local concentration measured with a TMA-selective microelectrode located about 100–150 μm from the release site. To maintain accurate spacing, both microelectrodes were glued together in a fixed array (Fig. 1A) and the spacing of the tips measured before and after each experiment using a microscope equipped with a graticule. The time-dependent rise and fall of the extracellular TMA^+ concentration during and after an iontophoretic pulse (TMA^+ diffusion curves) were fitted to a radial diffusion equation modified to account for extracellular volume fraction α , tortuosity λ and non-specific TMA^+ uptake k' (Nicholson & Phillips,

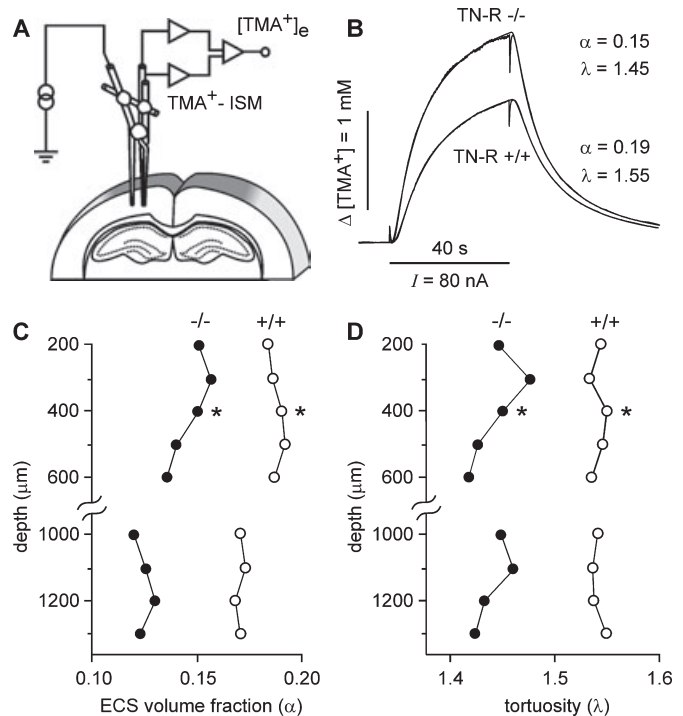


FIG. 1. Method for determining the extracellular space (ECS) volume fraction α and tortuosity λ in the mouse brain *in vivo*. (A) Schematic diagram of the experimental arrangement for diffusion measurements. Two microelectrodes, a double-barrelled tetramethylammonium (TMA^+)-selective microelectrode (TMA^+ -ISM) and a micropipette for TMA^+ iontophoresis, were glued together to enable the measurement of TMA^+ diffusion curves (concentration vs. time profiles). (B) TMA^+ diffusion curves were measured with the same microelectrode array in a pair of mice [tenascin (TN)-R^{-/-} and TN-R^{+/+}]. Thereafter, the curves were used to calculate α and λ . Note that the ECS volume fraction is lower and the diffusion curve shows a higher amplitude (i.e. a faster rise and fall time) in the TN-R^{-/-} mouse than in the control mouse. (C and D) Graphs showing the values of α and λ obtained along an individual microelectrode track. The asterisks highlight the values that correspond to the diffusion curves depicted in (B).

1981). If r is the distance between the tips of the source and ion-selective microelectrodes (ISM), $Q = n \times I/F$ (mol/s) is the iontophoresis source term, where I is the current, typically 180 nA, n is the transport number for TMA^+ and a specific iontophoresis electrode, and F is the Faraday constant, t is time after starting the iontophoretic pulse, and t_p is the duration of the iontophoretic pulse, then the TMA^+ concentration C (mM) is given by:

$$C(t) = \left(\frac{Q\lambda^2}{8\pi D\alpha r} \right) \exp \left[\left(r\lambda\sqrt{\frac{k'}{D}} \right) \operatorname{erfc} \left(\frac{r\lambda}{2\sqrt{Dt}} + \sqrt{k't} \right) + \exp \left(-r\lambda\sqrt{\frac{k'}{D}} \right) \operatorname{erfc} \left(\frac{r\lambda}{2\sqrt{Dt}} - \sqrt{k't} \right) \right] \quad (1)$$

for $t \leq t_p$,
and

$$C'(t) = C(t) - C(t - t_p) \text{ for } t > t_p. \quad (2)$$

In brief, Eq. (1) describes the increase in TMA^+ concentration during the current source pulse; Eq. (2) is complementary to Eq. (1) and describes the decay in the TMA^+ concentration after the end of the current pulse. Diffusion curves were first recorded in 0.3% agar gel

made up in 150 mM NaCl, 3 mM KCl and 0.5–1.0 mM TMA chloride to calibrate the microelectrode array, i.e. to obtain the transport number n (an iontophoresis electrode characteristic) and the array spacing r . The transport number and array spacing can be determined by solving Eqs (1) and (2) because, by definition, in agar the diffusion parameters are $\alpha = 1$, $\lambda = 1$ and $k' = 0$. Thereafter, the recordings were done in layers III–VI of the cerebral cortex and in the CA1 region of the hippocampus to obtain the ECS diffusion parameters α , λ and k' . The calculations were done by fitting the diffusion curves to Eqs (1) and (2) using the SIMPLEX algorithm implemented in VOLTORO software (C. Nicholson, NYU School of Medicine, New York, USA).

Animals were deeply anaesthetized with sodium pentobarbital (90 mg/kg) administered intraperitoneally, a dose that is in compliance with NIH ARAC guidelines for mice. A supplemental dose of 30 mg/kg was given every additional hour. The cortex was exposed with 0.5 mm diameter trephination holes (1.5 mm lateral and 1.5 mm caudal to bregma), and the dura was gently removed from this opening. A stereotaxic apparatus (David Kopf Instruments, USA) was used to control the dorso-ventral and caudo-lateral positioning of the microelectrodes. The electrodes' penetration of the brain surface and their lowering into the brain were driven by a remote control micromanipulator (Nanostepper, SPI, Oppenheim, Germany). The assignment of cortical depths to cortical layers was done from subsequent histological data, taking into account slice shrinkage (about 5%). The slice shrinkage, caused by the histological procedure, was determined by comparing histological slices and *in vivo* MR images. The exposed cortex was washed with a solution containing 150 mM NaCl, 3 mM KCl and 0.5 mM TMA chloride at 37 °C. The solution serves to protect the brain and also as a reference for the TMA⁺ concentration. There is a drop in concentration when lowering the microelectrode into the brain, and therefore the surface of the brain can easily be determined. The TMA diffusion measurements were performed only along the mediolateral axis. These enabled us to determine the correct value of the tortuosity in this direction, but the measured value of the ECS volume fraction will be slightly different from the actual value in regions with diffusion anisotropy (Voříšek & Syková, 1997b), typically in the hippocampus. To obtain the actual value of the ECS volume fraction requires measurements to be performed along at least three axes. This point is not important for the current study, which compared two groups of animals looking for possible differences. During measurements, the animals were breathing spontaneously, placed on a heated pad to maintain body temperature at 37 °C.

DW-MRI

For MRI measurements the animals were anaesthetized with isoflurane (1.5% in a mixture consisting of 40% O₂ and 60% N₂O) and placed in a heated mouse holder; they breathed spontaneously. DW-MRI measurements were performed using an experimental MR spectrometer BIOSPEC 4.7 T system (Bruker, Ettlingen, Germany) equipped with a 200 mT/m gradient system (190 μ s rise time) and a homemade head surface coil. We acquired nine T_2 -weighted sagittal images (TE of 19 ms, TR of 2.4 s, four acquisitions, field of view 1.92×1.92 cm², matrix size 256×128 , slice thickness of 0.8 mm, interslice distance 0.8 mm) in order to position coronal slices. Six DW images per slice were acquired using the following parameters: $\Delta = 30$ ms, b -factors = 136, 329, 675, 1035, 1481 and 1825 s/mm², $TE = 46$ ms, $TR = 1200$ ms, field of view 1.92×1.92 cm², matrix size = 256×128 , four 0.8-mm-thick coronal slices, interslice

distance = 1.2 mm. DW images were measured using the stimulated echo sequence. DW serves to exaggerate the contrast in T_2 -weighted images for water diffusion. The b -factor denotes the strength of DW. The stronger the DW, the darker the images are in areas with fast water diffusion. In DW measurements, the diffusion gradient direction pointed along the rostrocaudal direction.

The reproducibility of apparent diffusion coefficient of water (ADC_w) measurements was verified by means of six diffusion phantoms placed on the top of the heads of the mice. The phantoms were made from glass tubes (inner diameter = 2.3 mm, glass type: KS80, Rückl Glass, Otovice, Czech Republic) filled with pure (99%) substances having different diffusion coefficients. The substances were: 1-octanol, n-tridecane (Sigma Aldrich, Steinheim, Germany), isoamyl alcohol, isopropyl alcohol, n-butanol and tert-butanol (Penta, Prague, Czech Republic). The temperature of the phantoms was maintained at a constant 37 °C.

Histology

Immediately after TMA diffusion measurements, the animals, under deep anaesthesia, were perfused transcardially with 0.1 M phosphate-buffered saline (pH 7.4) followed by buffered 4% paraformaldehyde (pH 7.4). Brains were removed and postfixed (24 h) in the same fixative, then stepwise saturated with sucrose. After freezing, 40- μ m serial coronal sections were cut on a freezing-sliding microtome and collected in 0.1 M TRIS-buffered saline (pH 7.4). The sections were then stained with Cresyl violet.

Data processing and statistical analysis

Measurements of the ECS diffusion parameters using the real-time iontophoretic TMA method were performed at several depths in one or two tracks within the somatosensory cortex and the hippocampus (1.5 mm posterior to bregma, 1.5 mm lateral to midline). All measurements performed either in the cortex or the hippocampus of an individual animal were averaged and the averages used for final statistics.

Maps of the apparent diffusion coefficients were calculated from six DW images, which correspond to six different b -factors, by fitting the decay signal intensities to Eq. (3) (Le Bihan & Basser, 1995). The signal intensity S decays with increasing DW (b -factor).

$$S(b) = S_0 \exp(-b \times ADC_w) \quad (3)$$

The ADC_w was assumed to be zero in pixels where the acquired data did not fit well to theoretical dependence (correlation coefficient was less than 0.2). These zero-values were ignored for statistical evaluation if they occurred in the region of interest. ADC_w maps (see Fig. 3) were calculated using custom-made software (V. Herynek, IKEM, Prague, Czech Rep.) by a linear least-square algorithm. The results were analysed using ImageJ software (W. Rasband, NIH, Bethesda, USA). The evaluated regions of interest were positioned using a mouse brain atlas (Franklin & Paxinos, 1997) and T_2 -weighted images in both the left and right hemispheres. The minimal area of an individual region was 1.5 mm². We evaluated two adjacent coronal slices (0.8–2.2 mm caudal to bregma) in each animal.

All data are presented as mean \pm SEM. Statistical analysis of the differences between groups was evaluated using a two-tailed Student's t -test (InStat, GraphPad Software, San Diego, USA). The differences were considered significant if $P < 0.05$. N represents the number of mice used.

TABLE 1. Diffusion parameters in TN-R^{-/-}, ST^{-/-} and TN-C^{-/-} mice and their respective controls (+/+)

Region and ECS parameter	TN-R ^{+/+}	ST ^{+/+} , TN-C ^{+/+}	TN-R ^{-/-}	ST ^{-/-}	TN-C ^{-/-}
Primary somatosensory cortex					
α	0.196 ± 0.005	0.192 ± 0.006	0.154 ± 0.010*	0.174 ± 0.005*	0.182 ± 0.007
λ	1.55 ± 0.01	1.52 ± 0.02	1.49 ± 0.02*	1.46 ± 0.01*	1.48 ± 0.02
k' (10 ⁻³ /s)	4.7 ± 0.4	5.0 ± 0.4	5.6 ± 0.8	4.5 ± 0.6	5.0 ± 0.5
(N)	(7)	(11)	(7)	(6)	(9)
CA1 region of the hippocampus					
α	0.170 ± 0.012	0.167 ± 0.007	0.125 ± 0.006*	0.141 ± 0.008*	0.155 ± 0.009
λ	1.57 ± 0.03	1.54 ± 0.01	1.48 ± 0.02*	1.49 ± 0.02*	1.52 ± 0.03
k' (10 ⁻³ /s)	3.3 ± 0.8	4.0 ± 0.6	3.0 ± 0.5	3.2 ± 0.5	3.5 ± 0.5
(N)	(5)	(8)	(5)	(6)	(5)

Extracellular space (ECS) volume fraction α , tortuosity λ and non-specific uptake k' were measured by the tetramethylammonium (TMA) method in the primary somatosensory cortex and CA1 region of the hippocampus. The measurements were performed along the mediolateral axis. Significant differences ($P < 0.05$) between deficient mice and their respective controls are marked with asterisks. N , number of animals. ST, sulphotransferase; TN, tenascin.

Results

The diffusion parameters α , λ and k' were measured *in vivo* by the TMA method using ISM. Measurements were done in the primary somatosensory cortex of adult mice at depths of 200, 300, 400, 500, 600 and 700 μm as well as in the CA1 region of the hippocampus at depths of 1000, 1100, 1200 and 1300 μm from the brain surface. Before data analysis, the sites of the measurements were verified histologically. It is important to note that the differences between knockout and wild-type mice that we found existed in all anatomical layers of the brain cortex and hippocampus, as shown in Fig. 1C and D, and that there were no significant differences in diffusion parameters among the cortical layers (III–VI). Therefore, the values of the diffusion parameters were pooled across all measured cortical layers and across depths of 1000–1300 μm (CA1 region of the hippocampus) (Table 1). The mean values obtained in control animals are within the range of values found in the rat cortex and hippocampus (for review, see Nicholson & Syková, 1998). There were no significant differences between TN-R^{+/+} mice and the unified group of ST^{+/+} and TN-C^{+/+} mice (Table 1).

In TN-R-deficient animals (TN-R^{-/-}), both the ECS volume fraction α and tortuosity λ were significantly decreased (Table 1). In comparison with TN-R^{+/+} animals, in the cortex α decreased by 22% (to about 0.15) and λ decreased to about 1.49, while in the hippocampus α decreased by 26% (to about 0.13) and λ decreased to about 1.48. In the cortex of ST^{-/-} mice, we found a decrease in α of 9% (to about 0.17) and λ decreased to 1.46. Similarly, in the hippocampus of ST^{-/-} mice α decreased by 16% (to about 0.14) and λ decreased to 1.49. In contrast, in TN-C^{-/-} animals we did not find a significant decrease in α or λ (Table 1). Non-specific uptake k' was not significantly changed in TN-R^{-/-}, TN-C^{-/-} or ST^{-/-} mice. Figure 1B shows examples of TMA⁺-diffusion curves in control and TN-R^{-/-} mice. Compared with the control mouse, the amplitude of the diffusion curve obtained in the TN-R^{-/-} mouse was increased due to a smaller ECS volume fraction. The faster increase and decrease of the diffusion curve obtained in the TN-R^{-/-} mouse reveals a lower ECS tortuosity (Fig. 1B). The observed changes in α and λ were present in all layers of the somatosensory cortex as well as in the CA1 region of the hippocampus (Fig. 1C and D). Figure 2 shows all data obtained in the cortex of TN-R^{+/+} and TN-R^{-/-} animals plotted against their quantile order. The median values show the same differences as the mean values.

To obtain reliable data in more anatomical regions, we used DW-MRI. In contrast to substances diffusing predominantly in the ECS (e.g. TMA⁺), water diffuses both in the intracellular and extracellular

compartments. ADC_W averages the contributions from these different subcompartments (Pfeuffer *et al.*, 1999). Previous studies have shown that changes in ADC_W may reflect changes in both ECS volume fraction and tortuosity (van der Toorn *et al.*, 1996; Voříšek *et al.*, 2002). We compared the mean values of ADC_W in five regions: in the motor cortex, primary and secondary somatosensory cortices, hippocampus and thalamus in deficient animals and in control animals (Fig. 3A and B shows regions of interest definition). The results are summarized in

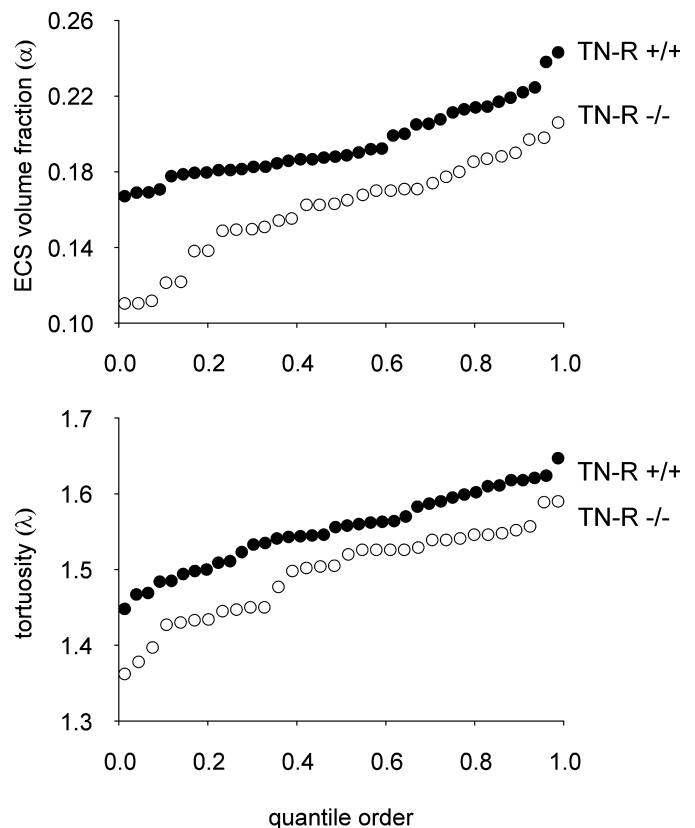


FIG. 2. Quantile plots of the extracellular space (ECS) volume fraction α and tortuosity λ in the cortex of tenascin (TN)-R^{-/-} mice and their respective controls. The data obtained in different mice at various depths were sorted according to their value and plotted in this order. The plots illustrate the significant reduction in ECS volume fraction and tortuosity found in TN-R^{-/-} mice.

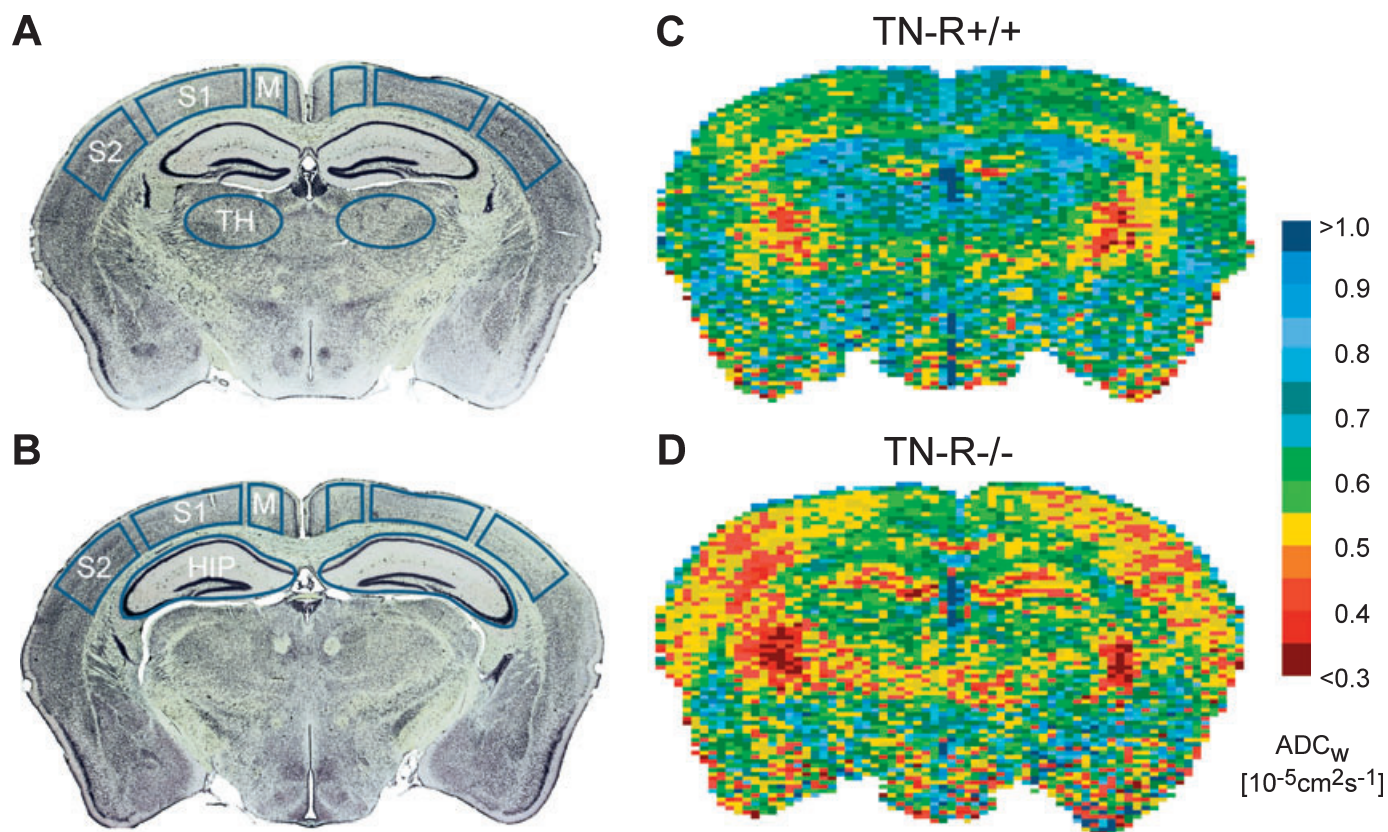


FIG. 3. Typical apparent diffusion coefficient of water (ADC_w) maps of tenascin (TN)-R+/+ and TN-R-/- mice. ADC_w was calculated in five selected areas: motor cortex (M), primary somatosensory cortex (S1), secondary somatosensory cortex (S2), hippocampus (HIP) and thalamus (TH). (A and B) The areas are outlined in the microphotographs of Cresyl violet-stained slices. (C and D) The images show ADC_w maps of TN-R+/+ and TN-R-/- mice; both images are from the same coronal plane as shown in (B). The scale at the bottom of the figure shows the relation between the intervals of ADC_w values and the colours used for visualization. Note the lower ADC_w throughout the whole slice from the TN-R-/- mouse when compared with the TN-R+/+ control.

Table 2. There was a significant decrease in ADC_w in all five regions in TN-R-/- as well as in ST-/- animals when compared with their respective controls. Similarly, as when using the TMA method, we did not find significant changes in ADC_w in TN-C-/- mice. In order to visualize the overall differences between different groups of animals, ADC_w maps were converted to pseudocolour images. Figure 3C and D shows a typical decrease in ADC_w in the entire brain of a TN-R-/- mouse, in which the average decrease of ADC_w throughout all measured regions was 8% when compared with controls.

To verify the quality of our MR measurements, we evaluated ADC_w in phantoms placed on top of the heads of TN-R-/-, TN-C-/- and ST-/- mice and their respective controls. We evaluated the phantom

measurements and did not find significant differences among these animal groups. The differences in ADC_w between any two individual measurements in phantoms were less than 5%, showing that our measurements of ADC_w were not affected by any systematic error.

Discussion

We used the real-time iontophoretic TMA method and DW-MRI to investigate the ECS diffusion parameters and tissue diffusivity in the cerebral cortex and hippocampus of TN-R-/-, TN-C-/- and ST-/- mice, and their respective controls. We found that an altered ECM results in a significant decrease in ECS volume fraction in TN-R-/-

TABLE 2. Apparent diffusion coefficient of water in TN-R-/-, ST-/- and TN-C-/- mice and their respective controls

Brain region	ADC_w ($\mu\text{m}^2/\text{s}$)				
	TN-R+/+ (<i>N</i> = 7)	ST+/+, TN-C+/+ (<i>N</i> = 8)	TN-R-/- (<i>N</i> = 8)	ST-/- (<i>N</i> = 8)	TN-C-/- (<i>N</i> = 6)
Motor cortex	689 ± 8	736 ± 8	634 ± 11*	676 ± 10*	757 ± 10
Primary somatosensory cortex	581 ± 10	608 ± 6	532 ± 9*	558 ± 7*	622 ± 5
Secondary somatosensory cortex	550 ± 11	566 ± 4	506 ± 10*	520 ± 6*	575 ± 7
Hippocampus	668 ± 8	705 ± 14	631 ± 8*	638 ± 10*	705 ± 11
Thalamus	513 ± 14	554 ± 21	460 ± 12*	464 ± 11*	526 ± 12

Apparent diffusion coefficient of water (ADC_w) was measured by diffusion-weighted magnetic resonance imaging (DW-MRI) and the values were evaluated in five brain regions (see Fig. 3). Significant differences ($P < 0.05$) between deficient mice and their respective controls are marked with asterisks; *N* = number of animals.

and ST^{-/-} mice. The decrease in TN-R^{-/-} animals probably reflects not only the loss of TN molecules, but also the loss of other components. Weber *et al.* (1999) found that in the brain of TN-R^{-/-} mice, staining for chondroitin sulphate proteoglycans and perineuronal nets is weak or more diffuse and abnormally distributed, e.g. it does not extend to the dendrites as in wild-type mice (Brückner *et al.*, 2000). The role of the ECM in determining ECS volume can also be demonstrated by the changes seen during development. Early postnatally, a high ECM content (Margolis *et al.*, 1975) is accompanied by higher values of the ECS volume fraction (Lehmenkühler *et al.*, 1993; Voříšek & Syková, 1997a). Other studies using the TMA method have indicated that the loss of ECM, fibronectin or chondroitin sulphate proteoglycan in aged animals coincides with a decrease in ECS volume fraction and tortuosity in these animals compared with young adults (Syková *et al.*, 1998). In particular, large changes were observed in the hippocampus of aged rats with impaired spatial learning compared with those with relatively preserved spatial memory (Syková *et al.*, 2002). The same relationship is also valid for many pathological states, e.g. astrogliosis, in which both an increased production of ECM molecules and an increased ECS volume fraction have been observed (Voříšek *et al.*, 2002).

The ECS tortuosity was also significantly decreased in TN-R- and HNK-1 ST-deficient mice. The correlation between ECS volume fraction (α) and tortuosity (λ) has been the subject of many discussions and theoretical models (Rusakov & Kullmann, 1998; Chen & Nicholson, 2000). The rapid decrease in ECS volume evoked by, for example, cell swelling during ischaemia, spreading depression or the application of hyposmotic solutions is accompanied by an increase in tortuosity (a decrease in the apparent diffusion coefficient) (Voříšek & Syková, 1997a; Kume-Kick *et al.*, 2002); and long-lasting changes in ECM content, e.g. during ageing or astrogliosis, may be accompanied by changes in α and λ in the same direction (Syková *et al.*, 1998; Voříšek *et al.*, 2002). Similarly as during ageing and in astrogliotic tissue, in TN-R-deficient mice we observed a decrease in both α and λ . We hypothesize that the tortuosity decrease in the present work is related to changes in the viscosity component (Rusakov & Kullmann, 1998) due to ECM defects. The obstacles in diffusion pathway could be cellular (the geometric component of tortuosity) or macromolecular (viscosity component). The geometric component changes when cells or their processes change their size or shape, i.e. during ischaemia or reactive gliosis. When only the geometric component is taken into account, the decrease in ECS volume seen in TN-R^{-/-} mice should lead to a tortuosity increase (Tao & Nicholson, 2004), not a decrease as seen in the measured animals. The concept of 'dead spaces' (Hrabětová & Nicholson, 2004), which can in certain experimental situations explain simultaneous decreases in α and λ , cannot be directly applied to TN-R knockouts without further validation, as the concept was demonstrated *in vitro* in experiments in which extracellular pores were blocked by large macromolecules. Therefore, it seems likely that the geometric component is not the cause of the observed tortuosity decrease in these animals.

The tortuosity apparently decreases due to a reduced number of obstacles in the diffusion pathway, e.g. missing TN-R molecules in the ECS. The tortuosity can be changed when the ECS structure is altered, e.g. when HNK-1 molecules are not sulphated in ST^{-/-} mice. The explanation for changes in the ECS volume fraction is more complex. We consider two hypotheses. First, the high density of negative charges carried by the ECM, especially by glycosaminoglycans, attracts osmotically active cations, such as Na⁺, causing large amounts of water to be drawn into the ECM. This creates a swelling pressure, or turgor, that enables the ECM to withstand compressive forces and leads to the expansion of the ECS (Alberts *et al.*, 1994). In TN-R^{-/-}

mice, a reduction in glycosaminoglycans, which retain water in the ECS, therefore leads to a diminished ECS volume. Second, the ECM can hold cells apart. In the adult brain, molecules of the lectican family of chondroitin sulphate proteoglycans are thought to interact with hyaluronan and TN-R to form a ternary complex (Dityatev & Schachner, 2003). Yamaguchi (2000) proposed that the hyaluronan-lectican-TN-R complex constitutes the core assembly of the adult brain ECM, which is found mainly in the pericellular spaces of neurons as perineuronal nets. If a component of the ECM is missing, e.g. TN-R, this structure is weakened and can collapse. This theory is supported by the decrease in ECS volume fraction also seen in ST^{-/-} animals. HNK-1 molecules anchor glycoproteins to the cell membrane. In ST^{-/-} animals, changes as subtle as the sulphation of the HNK-1 epitope have a measurable influence on the diffusion parameters (the ECS volume fraction and tortuosity decrease); however, they have less of an influence than the lack of TN-R molecules. It is therefore evident that the sulphation of the HNK-1 epitope changes ECM composition or structure. In future research, it would be interesting to compare regional variations in the ECS volume fraction with the distribution pattern of proteoglycan components and parvalbumin in the brain (Hendry *et al.*, 1988; Brückner *et al.*, 1994). In terms of ECS size regulation, the ECM could influence extrasynaptic transmission and therefore play a role in delimiting the functional properties of individual brain regions.

Our aim was to correlate the changes in ECS diffusion parameters with the results of DW-MRI to improve our understanding and interpretation of DW-MRI data. The TMA method cannot be used in humans to measure ECS diffusion parameters; however, DW-MRI is widely available as an adjunct to MRI scanners in regular clinical use and allows us to calculate ADC_W and thus detect diffusion changes occurring simultaneously in almost any brain region. The changes in ADC_W could be linked to changes in tortuosity (van der Toorn *et al.*, 1996). A decrease in tortuosity facilitates the ECS diffusion of all molecules (including water). However, we found not an increase but a decrease of ADC_W in TN-R^{-/-} animals compared with controls. ADC_W is therefore probably more affected by the decrease in the extracellular volume fraction in TN-R^{-/-} mice. Such correlation between ECS volume fraction and ADC_W is in agreement with previous studies (Voříšek *et al.*, 2002; Syková *et al.*, 2005). Indeed, in our experiments in TN-R^{-/-} mice the ECS volume fraction was decreased by 22–26%.

In contrast to substances diffusing predominantly in the ECS (e.g. TMA⁺), water diffuses both in the intracellular and extracellular compartments. ADC_W averages the contributions from these different subcompartments (Pfeuffer *et al.*, 1999). Previous studies have shown that changes in ADC_W may reflect changes in both ECS volume fraction and tortuosity (van der Toorn *et al.*, 1996; Voříšek *et al.*, 2002). The MR method measures an effective ADC_W with contributions from the diffusion properties of multiple subcompartments, e.g. the extra- and intracellular spaces. Using data from TMA measurements, we can estimate water diffusivity in the ECS. The tortuosity of the ECS is similar for small molecules (Nicholson & Syková, 1998), therefore we can estimate, using the tortuosity values obtained in TMA measurements, that the diffusion coefficient of water in the ECS ($ADC_W = D/\lambda^2$) is approximately 1500 $\mu\text{m}^2/\text{s}$ ($D = 3200 \mu\text{m}^2/\text{s}$ at 37 °C, $\lambda = 1.5$). The typical value of ADC_W in the tissue is less, about 600 $\mu\text{m}^2/\text{s}$. This indicates that in the cells, there is several-fold slower diffusion than in the ECS (to balance the higher diffusivity in the ECS). In summary, there are at least two subcompartments with significantly different diffusion properties. This poses difficulties for ADC_W interpretation, a problem that has still not been successfully resolved (Norris & Niendorf, 1995; Pfeuffer *et al.*, 1999; Kroenke &

Neil, 2004). However, if the volume ratio between them changes, the average water diffusion coefficient in the tissue (ADC_w) is affected (Voříšek *et al.*, 2002). Rather than changes in ECS diffusion barriers, the decrease in ADC_w reflects an increased ratio between the intra- and ECS volumes (van Gelderen *et al.*, 1994), and corresponds to the decrease in the ECS volume fraction.

Significant changes in ECS volume fraction, tortuosity and ADC_w were observed in both TN-R $-/-$ and ST $-/-$ mice. The lack of such changes in TN-C $-/-$ mice probably reflects the fact that whereas TN-R is one of the main components of the adult brain's ECM, TN-C expression in adulthood is not high enough to significantly modify the diffusion properties of the tissue, including regions that exhibit neuronal plasticity (hippocampus). In addition, we demonstrated that the lack of TN-C during development in TN-C $-/-$ mice did not influence the composition of the ECM in adulthood in such a way as to affect the diffusion parameters.

In conclusion, we found that modifications of ECM composition can change the diffusion parameters of the ECS. Therefore, the diffusion of neurotransmitters, trophic factors and ions (e.g. K^+ , Ca^{2+}) in the ECS is affected, which has direct functional implications. For example, in the CA1 region of the hippocampus, perineuronal nets are involved in the regulation of perisomatic inhibition, which is affected in TN-R $-/-$ mice (Gurevicius *et al.*, 2004). Härtig *et al.* (1999) proposed that perineuronal nets serve as rapid local buffers of excess cation changes in the ECS and that the effectiveness of this buffering depends purely on the diffusion parameters in the cell-surrounding ECM net. ECM molecules show diverse patterns of expression in different brain regions (Brückner *et al.*, 2003) that locally modify the diffusion parameters. When the diffusion parameters are changed in particular brain regions, we can postulate changes in signal transmission and behaviour. In the absence of the extracellular glycoprotein TN-R, the ECS volume fraction is greatly decreased and there is also a decrease in tortuosity. The ECM molecules are therefore important in determining the size of the ECS and, in addition, they form diffusion barriers in the ECS affecting the diffusion of neuroactive substances in brain tissue.

Acknowledgements

This study was supported by grants from the Grant Agency of the Czech Republic 309/04/0753, the Academy of Sciences of the Czech Republic AV0Z50390512, the Ministry of Education, Youth and Sports of the Czech Republic 1M0021620803, and the Deutsche Forschungsgemeinschaft CEZ:L17/98:00023001. We would like to express our thanks to Milan Hájek and James Dutt for their kind reading of the manuscript and their valuable comments, and to Achim Dahlmann for mice genotyping.

Abbreviations

ADC_w , apparent diffusion coefficient of water; DW, diffusion-weighted; ECM, extracellular matrix; ECS, extracellular space; HNK-1, human natural killer 1; ISM, ion-selective microelectrode; LTP, long-term potentiation; MRI, magnetic resonance imaging; ST, sulphotransferase; TMA, tetramethylammonium; TN, tenascin.

References

Alberts, B., Bray, D., Lewis, J., Raff, M., Roberts, K. & Watson, J. (1994) *Molecular Biology of the Cell*. Garland Science Publishing, New York.
 Bartsch, U., Pesheva, P., Raff, M. & Schachner, M. (1993) Expression of janusin (J1-160/180) in the retina and optic nerve of the developing and adult mouse. *Glia*, **9**, 57–69.
 Brückner, G., Grosche, J., Hartlage-Rübsamen, M., Schmidt, S. & Schachner, M. (2003) Region and lamina-specific distribution of extracellular matrix

proteoglycans, hyaluronan and tenascin-R in the mouse hippocampal formation. *J. Chem. Neuroanat.*, **26**, 37–50.
 Brückner, G., Grosche, J., Schmidt, S., Harting, W., Margolis, R.U., Delpech, B., Seidenbecher, C.I., Czaniera, R. & Schachner, M. (2000) Postnatal development of perineuronal nets in wild-type mice and in a mutant deficient in tenascin-R. *J. Comp. Neurol.*, **428**, 616–629.
 Brückner, G., Seeger, G., Brauer, K., Härtig, W., Kacza, J. & Bigl, V. (1994) Cortical areas are revealed by distribution patterns of proteoglycan components and parvalbumin in the Mongolian gerbil and rat. *Brain Res.*, **658**, 67–86.
 Bukalo, O., Schachner, M. & Dityatev, A. (2001) Modification of extracellular matrix by enzymatic removal of chondroitin sulfate and by lack of tenascin-R differentially affects several forms of synaptic plasticity in the hippocampus. *Neuroscience*, **104**, 359–369.
 Chen, K.C. & Nicholson, C. (2000) Changes in brain cell shape create residual extracellular space volume and explain tortuosity behavior during osmotic challenge. *Proc. Natl. Acad. Sci. USA*, **97**, 8306–8311.
 Dityatev, A. & Schachner, M. (2003) Extracellular matrix molecules and synaptic plasticity. *Nat. Rev. Neurosci.*, **4**, 456–468.
 Evers, M.R., Salmen, B., Bukalo, O., Rollenhagen, A., Bosl, M.R., Morellini, F., Bartsch, U., Dityatev, A. & Schachner, M. (2002) Impairment of 1-type Ca^{2+} channel-dependent forms of hippocampal synaptic plasticity in mice deficient in the extracellular matrix glycoprotein tenascin-C. *J. Neurosci.*, **22**, 7177–7194.
 Franklin, K.B.J. & Paxinos, G. (1997) *The Mouse Brain in Stereotaxic Coordinates*. Academic Press, San Diego.
 Fukamauchi, F., Wang, Y.J., Mataga, N. & Kusakabe, M. (1997) Paradoxical behavioral response to apomorphine in tenascin-gene knockout mouse. *Eur. J. Pharmacol.*, **338**, 7–10.
 Fuss, B., Wintergerst, E.S., Bartsch, U. & Schachner, M. (1993) Molecular characterization and in situ messenger RNA localization of the neural recognition molecule J1-160/180 – a modular structure similar to tenascin. *J. Cell Biol.*, **120**, 1237–1249.
 van Gelderen, P., de Vleeschouwer, M.H., DesPres, D., Pekar, J., van Zijl, P.C. & Moonen, C.T. (1994) Water diffusion and acute stroke. *Magn. Reson. Med.*, **31**, 154–163.
 Gurevicius, K., Gureviciene, I., Valjakka, A., Schachner, M. & Tanila, H. (2004) Enhanced cortical and hippocampal neuronal excitability in mice deficient in the extracellular matrix glycoprotein tenascin-R. *Mol. Cell. Neurosci.*, **25**, 515–523.
 Härtig, W., Brauer, K. & Brückner, G. (1992) Wisteria floribunda agglutinin-labelled nets surround parvalbumin-containing neurons. *Neuroreport*, **3**, 869–872.
 Härtig, W., Derouiche, A., Welt, K., Brauer, K., Grosche, J., Mader, M., Reichenbach, A. & Brückner, G. (1999) Cortical neurons immunoreactive for the potassium channel Kv3.1b subunit are predominantly surrounded by perineuronal nets presumed as a buffering system for cations. *Brain Res.*, **842**, 15–29.
 Haunsø, A., Ibrahim, M., Bartsch, U., Letiembre, M., Celio, M.R. & Menoud, P. (2000) Morphology of perineuronal nets in tenascin-R and parvalbumin single and double knockout mice. *Brain Res.*, **864**, 142–145.
 Hendry, S.H., Jones, E.G., Hockfield, S. & McKay, R.D. (1988) Neuronal populations stained with the monoclonal antibody Cat-301 in the mammalian cerebral cortex and thalamus. *J. Neurosci.*, **8**, 518–542.
 Hrabětová, S. & Nicholson, C. (2004) Contribution of dead-space microdomains to tortuosity of brain extracellular space. *Neurochem. Int.*, **45**, 467–477.
 Joester, A. & Faissner, A. (2001) The structure and function of tenascins in the nervous system. *Matrix Biol.*, **20**, 13–22.
 Jones, P.L. & Jones, F.S. (2000) Tenascin-C in development and disease: gene regulation and cell function. *Matrix Biol.*, **19**, 581–596.
 Keilhauer, G., Faissner, A. & Schachner, M. (1985) Differential inhibition of neurone-neurone, neurone-astrocyte and astrocyte-astrocyte adhesion by L1, L2 and N-CAM antibodies. *Nature*, **316**, 728–730.
 Kroenke, C.D. & Neil, J.J. (2004) Use of magnetic resonance to measure molecular diffusion within the brain extracellular space. *Neurochem. Int.*, **45**, 561–568.
 Kume-Kick, J., Mazel, T., Voříšek, I., Hrabětová, S., Tao, L. & Nicholson, C. (2002) Independence of extracellular tortuosity and volume fraction during osmotic challenge in rat neocortex. *J. Physiol.*, **542**, 515–527.
 Le Bihan, D. & Basser, P.J. (1995) Molecular diffusion and nuclear magnetic resonance. In Le Bihan, D. & Basser, P.J. (Eds), *Diffusion and Perfusion Magnetic Resonance Imaging: Applications to Functional MRI*. Raven Press, New York, pp. 5–17.
 Lehmenkühler, A., Syková, E., Svoboda, J., Zilles, K. & Nicholson, C. (1993) Extracellular space parameters in the rat neocortex and subcortical white

- matter during postnatal development determined by diffusion analysis. *Neuroscience*, **55**, 339–351.
- Margolis, R.K., Margolis, R.U., Preti, C. & Lai, D. (1975) Distribution and metabolism of glycoproteins and glycosaminoglycans in subcellular fractions of brain. *Biochemistry*, **14**, 797–804.
- Nakic, M., Manahan-Vaughan, D., Reymann, K.G. & Schachner, M. (1998) Long-term potentiation in vivo increases rat hippocampal tenascin-C expression. *J. Neurobiol.*, **37**, 393–404.
- Nicholson, C. & Phillips, J.M. (1981) Ion diffusion modified by tortuosity and volume fraction in the extracellular microenvironment of the rat cerebellum. *J. Physiol. (Lond.)*, **321**, 225–257.
- Nicholson, C. & Syková, E. (1998) Extracellular space structure revealed by diffusion analysis. *Trends Neurosci.*, **21**, 207–215.
- Norris, D.G. & Niendorf, T. (1995) Interpretation of DW-MR data: dependence on experimental conditions. *NMR Biomed.*, **8**, 280–288.
- Pesheva, P. & Probstmeier, R. (2000) The yin and yang of tenascin-R in CNS development and pathology. *Prog. Neurobiol.*, **61**, 465–493.
- Pfeuffer, J., Provencher, S.W. & Gruetter, R. (1999) Water diffusion in rat brain in vivo as detected at very large b values is multicompartmental. *MAGMA*, **8**, 98–108.
- Rusakov, D.A. & Kullmann, D.M. (1998) A tortuous and viscous route to understanding diffusion in the brain. *Trends Neurosci.*, **21**, 469–470.
- Saga, Y., Yagi, T., Ikawa, Y., Sakakura, T. & Aizawa, S. (1992) Mice develop normally without tenascin. *Genes Dev.*, **6**, 1821–1831.
- Saghatelian, A.K., Dityatev, A., Schmidt, S., Schuster, T., Bartsch, U. & Schachner, M. (2001) Reduced perisomatic inhibition, increased excitatory transmission, and impaired long-term potentiation in mice deficient for the extracellular matrix glycoprotein tenascin-R. *Mol. Cell. Neurosci.*, **17**, 226–240.
- Schachner, M., Taylor, J., Bartsch, U. & Pesheva, P. (1994) The perplexing multifunctionality of janusin, a tenascin-related molecule. *Perspect. Dev. Neurobiol.*, **2**, 33–41.
- Senn, C., Kutsche, M., Saghatelian, A., Bosl, M.R., Lohler, J., Bartsch, U., Morellini, F. & Schachner, M. (2002) Mice deficient for the HNK-1 sulfotransferase show alterations in synaptic efficacy and spatial learning and memory. *Mol. Cell. Neurosci.*, **20**, 712–729.
- Syková, E., Mazel, T., Hasenöhrl, R.U., Harvey, A.R., Šimonová, Z., Mulders, W.H. & Huston, J.P. (2002) Learning deficits in aged rats related to decrease in extracellular volume and loss of diffusion anisotropy in hippocampus. *Hippocampus*, **12**, 269–279.
- Syková, E., Mazel, T. & Šimonová, Z. (1998) Diffusion constraints and neuron–glia interaction during aging. *Exp. Gerontol.*, **33**, 837–851.
- Syková, E., Voříšek, I., Antonova, T., Meyer-Luehmann, M., Jucker, M., Hájek, M., Ort, M. & Bureš, J. (2005) Changes in extracellular space size and geometry in APP23 transgenic mice: a model of Alzheimer's disease. *Proc. Natl. Acad. Sci. USA*, **102**, 479–484.
- Tao, L. & Nicholson, C. (2004) Maximum geometrical hindrance to diffusion in brain extracellular space surrounding uniformly spaced convex cells. *J. Theor. Biol.*, **229**, 59–68.
- Theodosis, D.T., Pierre, K., Cadoret, M.A., Allard, M., Faissner, A. & Poulain, D.A. (1997) Expression of high levels of the extracellular matrix glycoprotein, tenascin-C, in the normal adult hypothalamoneurohypophysial system. *J. Comp. Neurol.*, **379**, 386–398.
- van der Toorn, A., Syková, E., Dijkhuizen, R.M., Voříšek, I., Vargová, L., Škobisová, E., van Lookeren Campagne, M., Reese, T. & Nicolay, K. (1996) Dynamic changes in water ADC, energy metabolism, extracellular space volume, and tortuosity in neonatal rat brain during global ischemia. *Magn. Reson. Med.*, **36**, 52–60.
- Voříšek, I., Hájek, M., Tintěra, J., Nicolay, K. & Syková, E. (2002) Water ADC, extracellular space volume, and tortuosity in the rat cortex after traumatic injury. *Magn. Reson. Med.*, **48**, 994–1003.
- Voříšek, I. & Syková, E. (1997a) Ischemia-induced changes in the extracellular space diffusion parameters, K^+ and pH in the developing rat cortex and corpus callosum. *J. Cereb. Blood Flow Metab.*, **17**, 191–203.
- Voříšek, I. & Syková, E. (1997b) Evolution of anisotropic diffusion in the developing rat corpus callosum. *J. Neurophysiol.*, **78**, 912–919.
- Weber, P., Bartsch, U., Rasband, M.N., Czaniara, R., Lang, Y., Bluethmann, H., Margolis, R.U., Levinson, S.R., Shrager, P., Montag, D. & Schachner, M. (1999) Mice deficient for tenascin-R display alterations of the extracellular matrix and decreased axonal conduction velocities in the CNS. *J. Neurosci.*, **19**, 4245–4262.
- Yamaguchi, Y. (2000) Lecticans: organizers of the brain extracellular matrix. *Cell. Mol. Life Sci.*, **57**, 276–289.